

Full Length Article

Effects of n-heptane/toluene/ethanol ternary fuel blends on combustion, operating range and emissions in premixed low temperature combustion

Ahmet Böğrek^a, Can Haşimoğlu^b, Alper Calam^{c,*}, Bilal Aydoğan^d

^a Ondokuz Mayıs University, Yeşilyurt Demir Çelik Vocational High School, Department of Automotive Technology, Samsun, Turkey

^b Sakarya University of Applied Science, Faculty of Technology, Department of Mechanical Engineering, Sakarya, Turkey

^c Gazi University, Technical Education Vocational High School, Department of Machine and Material Technology, Ankara, Turkey

^d Bandırma Onyedli Eylül University, Maritime Vocational High School, Department of Ship Construction, Balıkesir, Turkey



ARTICLE INFO

Keywords:

Toulene
Ethanol
Combustion
Fuel
Performance
Low temperature combustion

ABSTRACT

Low temperature combustion engines are a new combustion model that the reduction of nitrogen oxide emissions and the increasing of the thermal efficiency can be observed simultaneously. In addition, the problem of misfire at low engine loads and knocking at high engine loads occurs. The fuels have low octane number can be used to eliminate the misfire problem at low engine loads, and the fuels have high octane number can be used to eliminate knocking problem at high engine loads. In this study, the operating ranges of low and high reactivity fuel mixtures with different chemical properties were experimentally investigated in a low temperature combustion engine. While high reactivity n-heptane, T10 and E10 fuels were used, it was seen to be suitable for HCCI strategy in wider and leaner mixing conditions, while low reactivity E20 and E30 showed good performance at high engine loads close to the knocking zone. The highest brake thermal efficiency was obtained as 44.5% with E30 fuel under extremely lean mixture conditions ($\lambda = 2.95$). While E20 fuel shows a good performance like E30, the fact that most of the combustion takes place before TDC in the use of high reactivity fuel caused low efficiency due to knock and heat losses. It can be stated that ethanol has low reactivity needs high inlet air temperature, high compression ratio or combustion improving additives such as n-heptane and toluene to be used in HCCI applications. The results obtained support the idea of fuel flex vehicles for the current engine.

1. Introduction

The rapid growth of the industry increases the energy requirement and this causes the pollution of the atmosphere, soil and clean water resources rapidly [1–5]. For this reason, the need for clean and renewable energy is gaining importance day by day. It is predicted that the use of electric motors in the automotive sector will become widespread in the near future due to their zero emission advantage [6–8]. Despite the development of electric vehicle technology, the use of diesel engines in heavy-duty vehicles will continue. That's why, researchers keep working on new combustion modes providing lower emission values in existing internal combustion engines [9–14].

Homogeneous charge compression ignition (HCCI) engine is the new mode of combustion which has no spark plug or injector to start the combustion has high thermal efficiency and very low nitrogenoxide (NO_x) and particulate matter emissions [15–17]. Combustion starts

when the charge mixture reaches to chemical activation energy in this technology [18]. HCCI engines are operated more stably at partial loads. However, the temperatures of the gasses after HCCI combustion decreases and misfiring problem occurs at low engine loads [19]. Besides, there is a knocking problem at high engine loads. The simultaneous rapid combustion results in pressure fluctuations in HCCI combustion. Whole fuel taken into the cylinder is included in the combustion. So, knocking occurs [20–22]. Combustion must be decelerated to overcome this problem [23–25]. Exhaust gas recirculation (EGR) or negative valve thrust can be used to decelerate the combustion in HCCI engines [25–27]. Besides, the alcohols have high octane number can also decelerate the combustion [28]. A number of researchers have investigated the ways to eliminate misfiring and knocking problems of HCCI engines. Li et al. [29], examined the effect of n-butanol/n-heptane blends on knocking tendency and cyclical variations of an HCCI engine. It was reported that knock tendency decreased when the amount of n-butanol was increased in the blend. However, increasing both intake

* Corresponding author.

E-mail addresses: ahmet.bogrek@omu.edu.tr (A. Böğrek), canhasim@subu.edu.tr (C. Haşimoğlu), acalam@gazi.edu.tr (A. Calam), baydogan@bandirma.edu.tr (B. Aydoğan).

<https://doi.org/10.1016/j.fuel.2021.120628>

Received 20 August 2020; Received in revised form 21 January 2021; Accepted 4 March 2021

Available online 20 March 2021

0016-2361/© 2021 Elsevier Ltd. All rights reserved.

Nomenclature			
BSEC	Break specific energy consumption	HCCI	Homogeneous charge compression ignition
BTE	Break thermal efficiency	HRR	Heat release rate
CA	Crank angle	imep	Indicated mean effective pressure
CO	Carbonmonoxide	MPRR	Maximum pressure rise rate
E10	%10 toluene, %10 ethanol and %80 n-heptane blends	NOx	Nitrogenoxide
E20	%10 toluene, %20 ethanol and %70 n-heptane blends	PODE	Polyoxymethylene dimethyl ethers
E30	%10 toluene, %30 ethanol and %60 n-heptane blends	RI	Ringintensity
EGR	Exhaust gas recirculation	SFC	Specific fuel consumption
H100	Neat n-heptane	SI	Spark ignited engine
HC	Hydrocarbon	SOC	Start of combustion
		T10	%10 toluene and %90 n-heptane blends
		TDC	Top dead center

temperature and engine speed resulted in knocking combustion. Bahri et al [30], investigated how ethanol and n-heptane blends effect misfiring and knocking. They used a 0.3 L converted diesel engine. The results showed that ringing intensity (RI) decreased with the increase of CA50 and the decrease of combustion duration. Wang et al [31], conducted the effect of polyoxymethylene dimethyl ethers (PODE) on combustion by varying charge mass, lambda and EGR in HCCI engine. It was found that the decreasing lambda value resulted in decreasing of the combustion temperature and ignition timing of low temperature heat release delayed. The ignition timing of high temperature heat release advanced with the increase of equivalence ratio at the EGR ratio below 42%. Bahri et al [32], investigated the misfiring of the HCCI engine fuelled with ethanol. They found that start of combustion (SOC) and the crank angle (CA) where the maximum in-cylinder pressure is observed are not the important parameters for misfiring detection. However, they reported that variation of in-cylinder pressure strongly effected the misfiring at 5, 10, 15 and 20 CA after top dead center (TDC). Çınar et al [33], studied the effects of intake and exhaust valve lift on HCCI combustion fuelled with isooctane and n-heptane. They used one single cylinder gasoline engine in their experiments and varied the valve mechanism. The experiments showed that using cams with low lift could extend the operating range of the engine on knocking and misfiring zones. The increase of intake air temperature resulted in provided HCCI combustion at leaner mixture conditions. Starck et al [34], studied the performance and the emissions of HCCI engine fuelled with the various fuels with different cetane numbers. They used Jet B as a reference fuel in a direct injection, single cylinder, four stroke diesel engine in their experiments. They demonstrated that HCCI operating range can be extended more than 30% with the fuels have low cetane number and high volatility with appropriate chemical composition. Machrafi et al [35], investigated the effects of toluene on HCCI auto-ignition process. They performed the experiments between 25 and 120 °C inlet air temperature, 0.18 and 0.53 equivalence ratios and 6–13.5 compression ratios. They reported that toluene significantly delayed the ignition compared to n-heptane. Lee et al. [36], studied the effects of toluene addition into the diesel fuel and investigated the combustion characteristics of diesel engine. They found that the air–fuel mixing was enhanced with the addition of toluene. The ignition was also retarded with the usage of toluene. In previous studies, it had been pointed out that operating range of the HCCI engine got narrow with the addition of ethanol [37]. In summary, it has been shown from this review that the effects of toluene addition have not been closely examined with ethanol which has very high latent evaporation heat. This is one of the first study to undertake a detailed combustion analysis of toluene addition into the n-heptane/ethanol blends and also the operating ranges of the blends were investigated. At this purpose, the operating range, in-cylinder pressure, heat release rate (HRR), in-cylinder gas temperature, combustion duration, RI, CA10, BTE, CA50, imep, maximum pressure rise rate (MPRR), carbonmonoxide (CO) and hydrocarbon (HC) emissions were examined. The experiments were performed at constant 1000 rpm engine speed, 350 K intake air

temperature and varied lambda values.

2. Experimental setup

All the experiments were carried out using four stroke, a single cylinder, Ricardo Hydra spark ignited (SI) test engine. The engine setup and the properties of the test engine were given at Fig. 1 and Table 1, respectively. DC dynamometer which can absorb 30 kW power at 6500 rpm was connected to the test engine. The parameters such as engine load, speed, injection pulse and ignition were controlled with dynamometer control panel. K-type thermocouple which was coupled to exhaust line was used to measure exhaust gas temperature.

The lambda values were measured between 2.25 and 3.8 during the experiments. The engine speed was 1000 rpm and intake air temperature was held at 350 K. Kistler 6121 piezoelectric pressure sensor which of the technical properties were given at Table 2 was used to measure the in-cylinder pressure. Engine speed and top dead center were determined with the encoder which produces 1000 pulses per rotation. The pressure signals were amplified with Cussons P4110 combustion analyzer apparatus. Analog signals of pressure data were converted to digital signals with National Instrument data acquisition card. HRR, CA10, CA50 and etc. were computed with the MATLAB program using the in-cylinder pressure data which were recorded to the computer. Consecutive 50 cycles were averaged to eliminate cyclic variations. Five test fuels of which the compositions were given at Table 3 were used in the experiments. The properties of the test fuels were given at Table 4. Test fuels were prepared by mixing with a mechanical mixer before testing. It was then observed for 48 h that phase separation did not occur. During the experiments, mixed fuels were injected into the intake manifold with a low pressure (2.8 bar) single hole gasoline injector.

Lambda HC and CO were determined with Bosch BEA350 exhaust gas analyzer. The specifications of the gas analyzer were given at Table 5. The charge mixture taken into the cylinder was assumed as ideal gas while determining the heat release rate according to the first law of the thermodynamics. HRR was determined with the Eq. (1).

$$\frac{dQ}{d\theta} = \frac{k}{k-1} P \frac{dV}{d\theta} + \frac{1}{k-1} V \frac{dP}{d\theta} + \frac{dQ_{heat}}{d\theta} \quad 1$$

Here, dQ , $d\theta$, k , dQ_{heat} , represents the heat release, CA, the ratio of specific heat and the heat transfer to the cylinder wall, respectively. Network was calculated with the Eq. (2). Imep is an important parameter which defines the engine performance. Imep was calculated with the Eq. (3). Equation (4) was used to determine the indicated thermal efficiency.

$$W_{net} = \int P dV \quad 2$$

$$imep = \frac{W_{net}}{V_d} \quad 3$$

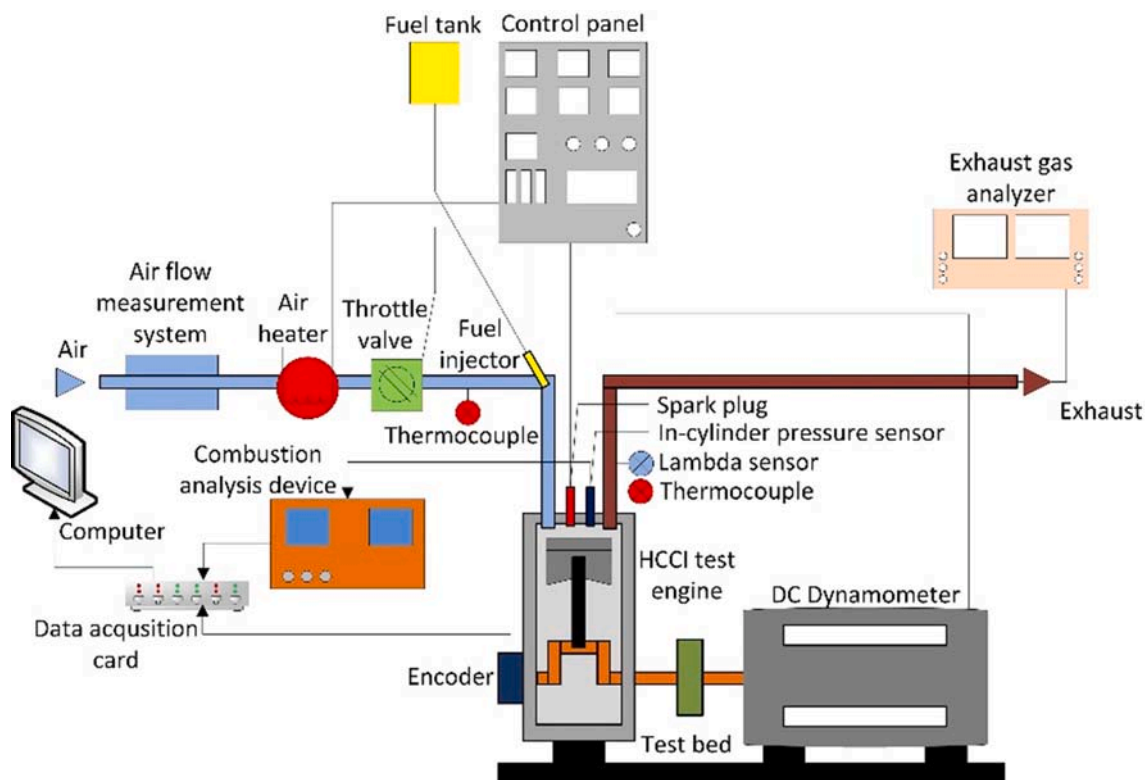


Fig. 1. HCCI engine setup.

Table 1
Test engine specifications.

Model	Ricardo-Hydra
Number of Cylinders	1
Stroke (mm)	88.9
Cylinder bore (mm)	80.26
Maximum engine speed (rpm)	5400
Volume (cc)	540
Compression ratio	13:1
Valve lift (mm)	Intake/exhaust 5.5/3.5
Valve timing	IVO/EVC 12° BTDC/56° ATDC

Table 2
Technical properties of the Kistler 6121 piezoelectronic transducer.

	Operating range
Operating range (bar)	0–250
Operating temperature (°C)	–50 to 350
Accuracy (±%)	0.5
Measurement precision (pC/bar)	14.7

Table 3
The compositions of the test fuels.

	n-Heptane (%)	Toluene (%)	Ethanol (%)
H100	100	–	–
T10	90	10	–
E10	80	10	10
E20	70	10	20
E30	60	10	30

Table 4
The properties of the test fuels.

	n-Heptane [10]	Toluene [38]	Ethanol [38,39]
Chemical formula	C ₇ H ₁₆	C ₇ H ₈	C ₂ H ₅ OH
Density (kg/m ³)	679.5	866	789
RON	0	120	92
Heat of combustion (kJ/mol)	4817	3910.3	1360
Self-ignition temperature (°C)	204	530	420
Boiling point (°C)	98	110.6	78.4
Molar mass (g/mol)	100.16	92.14	46.06

Table 5
The specifications of the Bosch BEA 350.

	CO (%) vol)	CO ₂ (%) vol)	HC (ppm)	O ₂ (%) vol)	λ	NO (ppm)
Operating range	0–10	0–18	0–9999	0–22	0.5–9.999	0–5000
Accuracy	0.001	0.01	1	0.001	0.001	1

$$\eta_T = \frac{W_{net}}{m_{fuel1} \cdot Q_{LHV1} + m_{fuel2} \cdot Q_{LHV2}} \quad 4$$

3. Test procedures

The test engine was run in SI mode before starting experimental work. When the engine coolant and lubricating oil temperature reached about 50 °C, the ignition system was turned off on the control panel and the spontaneous HCCI combustion was provided. The amount of fuel to be sprayed has been changed using the potentiometer located on the control panel and controlling the opening time of the injector in the port injection system. Thus, HCCI combustion at different lambda values was investigated in the range of knocking and misfiring boundary

conditions. It was determined that during the combustion of HCCI, the temperature of cooling water and lubricating oil was fixed at 70 °C and 55 °C respectively, before starting to record data. All experimental work was carried out under these conditions and the data were recorded. The intake air inlet temperature was fixed at 350 K.

4. Results and discussion

Fig. 2 shows the effects of toluene and ethanol addition into the n-heptane fuel on HCCI operating range. The scales of engine speed and

lambda were divided into equal segments for better comparison of the operating maps. Besides, the colors of the imep column are the same for all operating maps. The knocking and misfiring limits can be clearly seen from the Fig. 2. The highest engine speed which was the HCCI combustion was achieved was 2000 rpm for E20 fuel due to the insufficient time for the combustion of the air/fuel mixture at high engine speeds. When the Fig. 2 was mentioned that the addition of 10% toluene into the n-heptane has no significant effect on the operating range. The operating range was extended especially for E10 and E20 due to the better evaporation properties by adding toluene. The largest operating range

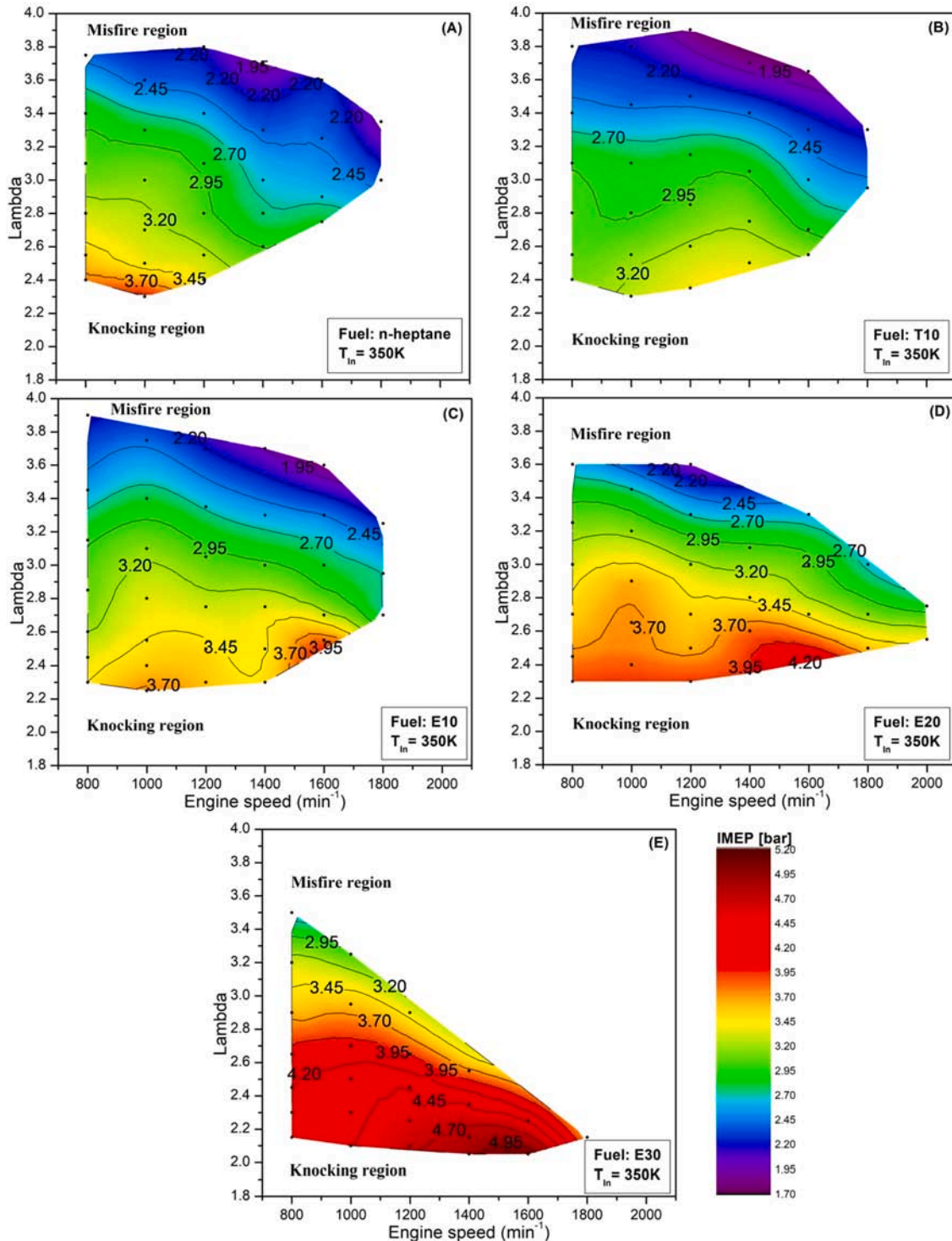


Fig. 2. Operating ranges of test fuels A) H100 B) T10 C) E10 D) E20 E) E30.

and the highest engine speed was observed for E20 fuel. Toluene can be used as combustion improver in HCCI engines fuelled with ethanol. The operating range of E30 fuel got narrower due the low reactivity properties of the ethanol.

Imep defines the average pressure exerted on the piston during one cycle and is an important parameter to determine the engine performance [40]. The addition of toluene into the n-heptane decreased imep. This phenomena can be explained with the increase of knocking by the high reactivity of toluene and n-heptane. The addition of low-reactivity ethanol into the n-heptane-toluene blend increased imep by controlled deceleration of the combustion. The resistance of the knocking increased with the addition of ethanol into the n-heptane/toluene blend. The octane number of the blends increases with increasing the amount of ethanol in the blend. So, HCCI combustion occurs slower and controllable. The maximum imep was observed as 5.05 bar for E30 fuel at 1600 rpm engine speed. Besides, the maximum imep values were obtained for E30 for all lambda values. As it can be seen from the Fig. 3 that the large

part of the heat release occur after TDC, thus thermal efficiency and imep increase synchronously.

Fig. 3 displays the variations of in-cylinder pressure and HRR of H100, T10, E10, E20 and E30 versus lambda while the engine speed was 1000 rpm. From the graph below we can see that knocking tendency disappears when the lambda value increases. This finding might be explained by the fact that fuel energy decreases which cause the decrease of HRR at higher lambda values. The fact remains that increasing amount of ethanol in the mixture decreased knocking. It is possible that this result is due to lower boiling point of the ethanol. So, heat increased during the combustion. It can be clearly seen from the Fig. 3 that in-cylinder pressure decreases with the increase of lambda. Similarly, HRR values were decreased when the lambda value increased. The variations of in-cylinder pressure and heat release of T10 test fuel at 1000 rpm engine speed between knocking and misfiring boundaries were given at Fig. 3b. There was no big difference between T10 and H100. But, it can be seen from the Fig. 3c-d and e ethanol directly effects

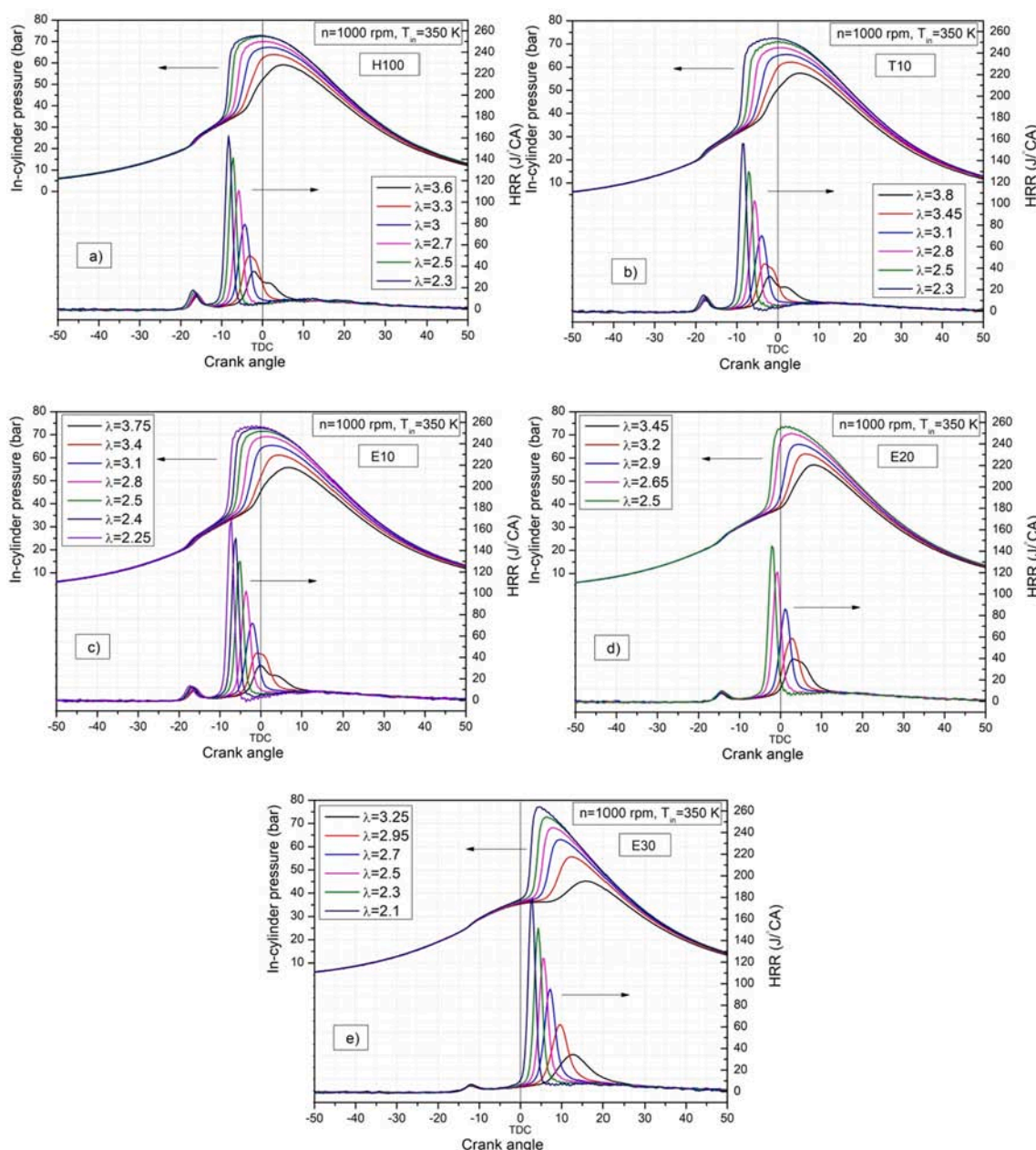


Fig. 3. The in-cylinder pressure and HRR of test fuels a) H100 b) T10 c) E10 d) E20 e) E30.

the combustion. E30 fuel which contains 30% ethanol provided for the combustion at richer conditions. Besides, combustion was retarded for all lambda values. This effect may be explained with higher octane number and latent heat of vaporization of ethanol. High octane number causes the negative temperature coefficient zone to elongate. More time for the evaporation of E30 is needed. The SOC is delayed in this duration. Especially in the use of H100, T10 and E10 fuels, it is seen that most of the heat release occurs before the TDC. This situation results in decrease of maximum in-cylinder pressure. It is seen that in the use of E30 fuel, despite the low lower heat value of ethanol, the maximum cylinder pressure is achieved. The main reason for this is that the most heat release occurs after the TDC. The maximum in-cylinder pressure of E30 was 77.5 bar at lambda = 2.1. The addition of ethanol into the mixture controls the combustion and maintained the large part of the heat release to occur after the TDC.

Fig. 4 displays an overview of the in-cylinder gas temperature of test fuels at $\lambda = 2.5$ and 1000 rpm. From the data in Fig. 4 it is apparent that in-cylinder gas temperature decreased for T10 and E10. Heating value and the combustion phasing are one of the most important parameters which effects the in-cylinder gas temperature. Ethanol and toluene have lower heating value than n-heptane. The minimum in-cylinder gas temperature was obtained on 10% toluene addition into the n-heptane. Heat release rapidly occurs BTDC with the usage of T10 fuel due to the evaporation of toluen quickly. This, increases the heat losses from the cylinder walls. Combustion was retarded with the addition of ethanol into the mixture at the same lambda values. The oxidation reactions were improved especially with the usage of E30 fuel. Consequently, maximum in-cylinder gasses temperature obtained at later CA's and with higher values.

CA10 value, which will be referred as the SOC in this study, is an important parameter in HCCI combustion, because the self ignition can not be controlled in HCCI [41,42]. If we could focus for a moment on Fig. 5 we can see that CA10 value increased with increasing the amount of ethanol in the mixture and there was no significant difference with the addition of toluene when compared to n-heptane. The CA10 values of H100, T10, E10, E20 and E30 were 8.64 °CA (before TDC), 8.28 °CA (before TDC), 6.48 °CA (before TDC), 3.24 °CA (before TDC) and 3.6 °CA (after TDC) respectively, at $\lambda = 2.5$. Evaporability and the octane number are the major parameters which effects the SOC in HCCI engines. Besides, the residual gasses remained from the previous cycle markedly effects the SOC. It can be clearly seen from the Fig. 5 that SOC was delayed with the increase of ethanol into the mixture at the same lambda values and engine speeds. The required conditions to start of the combustion into the cylinder obtained later due to the higher latent heat of vaporization of the alcohol. So, combustion is delayed. However, CA10 was retarded for all test fuels with the increase of lambda. The

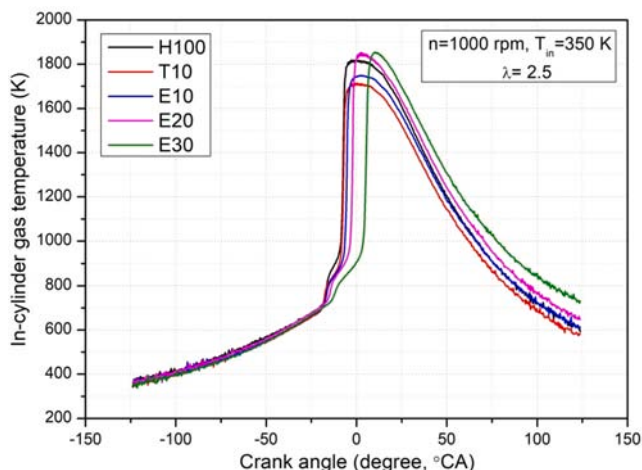


Fig. 4. The in-cylinder gas temperature of test fuels at constant lambda.

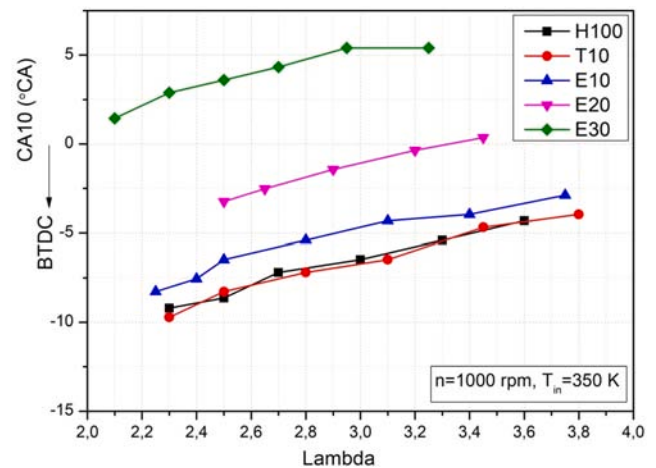


Fig. 5. CA10 of test fuels.

leaner the mixture, the worse the in-cylinder conditions in spontaneous HCCI combustion. The temperatures of the in-cylinder gasses decrease and fuel evaporates hardly. Low in-cylinder gasses temperature cause the HCCI combustion occur at later CA's. The latest HCCI combustion was observed for E30 among all the test fuels due to the higher octane number and low evaporability at all lambda values. In the other words, ethanol has a significant effect on the SOC.

The variations of brake thermal efficiency (BTE) and CA50 were given at Fig. 6a and b, respectively. The experiments were performed at 1000 rpm engine speed. The BTE is directly affected by the position of CA50 [43]. The maximum BTE is observed at the point where the CA50 is 7–10 °CA after TDC. As it can be seen from Fig. 6a CA50 is delayed when the mixture got leaner because of the similar results of CA10. In rich conditions, the probability of combining fuel molecules moving in the cylinder with oxygen increases. So, CA50 is advanced. It was observed that CA50 is obtained before TDC for all lambda values with the usage of H100 and T10. The rapid evaporation of heptane and toluene causes most of the combustion to occur before TDC. So, the negative force exerted on the piston increases. So the BTE decreases. The addition of ethanol into the mixture increases and delays the combustion duration. In spite of the fact that E30 has lower heat of combustion than the other test fuels the maximum BTE observed for E30. The maximum BTE was observed as 38.1% with E30 at lambda = 2.95. CA50 was observed at 10.5 °CA after TDC under these conditions. The maximum BTEs of H100, T10, E10 and E20 fuels were 34.9%, 33.6%, 36.9% and 37.5%, respectively, at 3.3, 3.1, 3.4 and 3.2 lambda values.

Indicated mean effective pressure (imep) is defined as the in-cylinder pressure exerted on the piston during a cycle [44,45]. Fig. 7 shows the variation of imep versus 50 cycle at $\lambda = 2.5$ at 1000 rpm. It can be clearly seen from the Figure that T10 and E30 showed the lowest and highest imep values, respectively. Ignition is controlled by chemical kinetics in HCCI combustion. Therefore, the type of fuel and lambda values are affected by the thermodynamic state of the mixture. There has been no physical mechanism controls the SOC in HCCI engines. More heat losses occurs especially in the regions close to the cylinder walls. Combustion may extinguish or it may not start at all. Unstable operation regions occur especially at high lambda values. Cyclic variations should not exceed 10% in internal combustion engines. The imep values of 50 cycles were given at Fig. 7. Unstable operation increased in the conditions which combustion occurred before TDC. The addition of ethanol into the mixture delayed the combustion and result in occur after TDC. This increases imep. The maximum imep was obtained with the usage of E30. The average imep was about 4.5 bar for E30 fuel.

Fig. 8 shows the change of brake torque and brake specific energy consumption (BSEC) depending on lambda. It can be seen in Fig. 8a that all test fuels in rich mixture regions provide high brake torque and lower

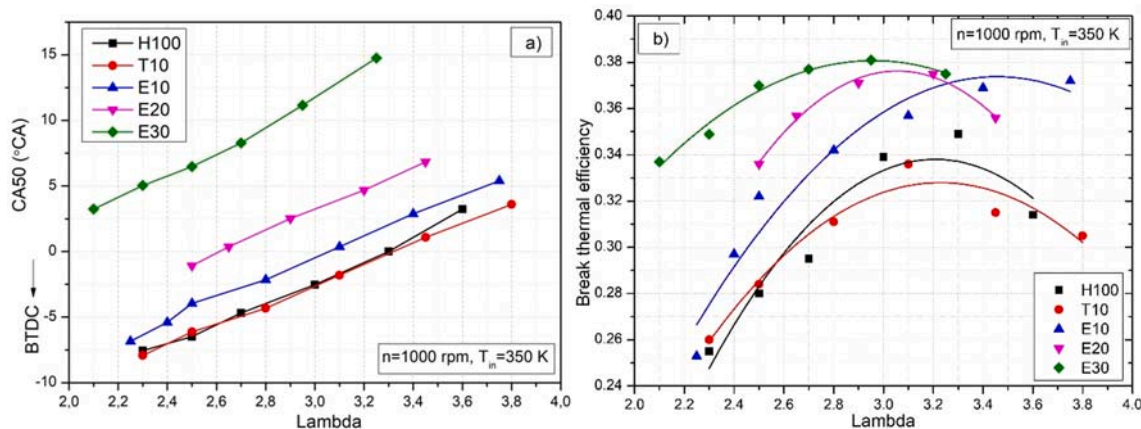


Fig. 6. The variations of a) CA50 and b) BTE.

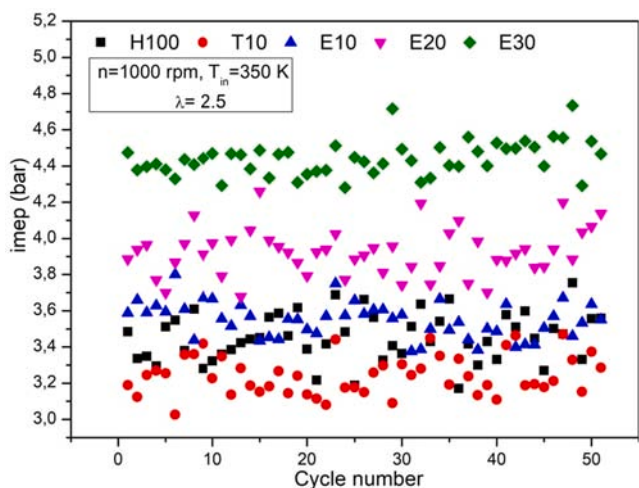


Fig. 7. The variations of imep for consecutive 50 cycles.

brake torque with the mixture getting poorer. In the rich mixing zones, more heat is released in the cylinder and the maximum in-cylinder pressure is achieved. Braking torque increases depending on the increase of the net work obtained by the piston. As the mixture becomes poorer, the amount of energy driven into the cylinder decreases, less heat energy is released and braking torque decreases. Brake torque variation of E30 fuel is different than other test fuels. The braking

torque is low at the richest mixing regions, but reaches to a maximum value at a optimum lambda value. Later, as the mixture becomes poor, the braking torque decreases again. The main reason for this is that ethanol’s latent heat of vaporization is very high. E30 fuel contains the highest rate (30%) of ethanol. When using E30 fuel in the rich mixture zone more fuel than other fuels is sent into the cylinder in mass. Therefore, the fuel evaporates longer. Some of the fuel can not be burned and the torque decreases, during the evaporation process. Maximum brake torque was recorded as 8.55 Nm with the use of E30 at $\lambda = 2.95$. As it can be clearly seen from the figure that brake torque has higher values when the amount of ethanol was increased in the blend. At the same engine load (same lambda value) the oxygen in ethanol improves combustion. Although it has a lower calorific value, ethanol is therefore seen as a promising fuel in internal combustion engines. However, when Fig. 7 is examined, it is seen that imep also increases depending on the amount of ethanol in mixed fuels. The increase in braking torque is related to imep [28,37,40,46–48].

When Fig. 6b is examined, it is seen that the maximum brake thermal efficiency is obtained in the use of E30 fuel under the same conditions. The ideal mixture ratio for E30 fuel was prepared under these conditions, the combustion efficiency increased and the braking torque increased. When the brake torque results due to lambda, especially for fuels with high reactivity (neat n-heptane and T10), are examined, minimum brake torque has been obtained at all lambda values. This is because highly reactive fuels start their in-cylinder oxidation reactions at earlier crank angles. Combustion is advanced and most of the combustion takes place before TDC. This reduces the net work done by the piston and braking torque is also reduced. Fig. 8b shows the variation of

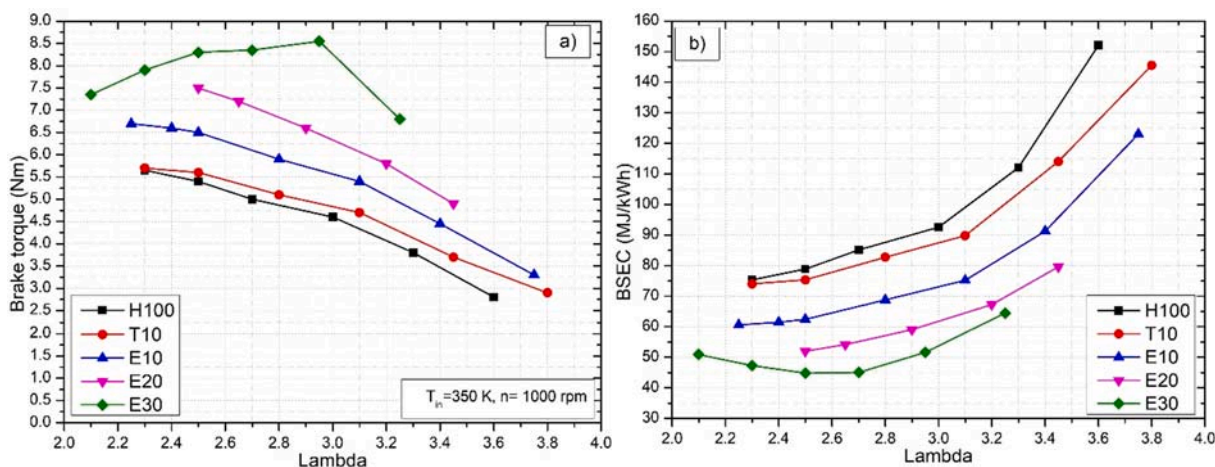


Fig. 8. The variations of a) Brake torque and b) BSEC.

break specific energy consumption (BSEC) depending on lambda. BSEC is the best choice for the analysis of blended fuels with different calorific values according to the specific fuel consumption display. In this study, the fuel with the highest calorific value is n-heptane which has the high reactivity. However, the rapid oxidation of n-heptane fuel increases negative work at all lambda values. Therefore, the highest BSEC values were obtained with the use of n-heptane. BSEC decreased due to the increase in the amount of ethanol in the mixture fuels and the lowest BSEC values were obtained by using E30 fuel. As the ethanol ratio in the mixture fuels increases, HCCI combustion slows down and the combustion is more controllable. It can be seen in Fig. 3e that a significant part of the combustion is obtained just after TDC, especially in the use of E30 fuel. The fast oxidation chemistry that occurs right after TDC improves combustion and increases brake thermal efficiency. In addition, oxygen content in ethanol also improves HCCI combustion. Thus, the combustion efficiency increases and BSEC decreases. The lowest BSEC was obtained with the usage of E30 fuel as 44.80 MJ/kWh at $\lambda = 2.7$. Combustion worsens in extremely lean mixture conditions in HCCI engines. For this reason, most of the energy put into the cylinder cannot be converted into effective efficiency. BSEC is very high in extremely lean mixing conditions.

Fig. 9 depicts the variations of RI and MPRR versus lambda at 1000 rpm. RI decreased when the mixture got leaner. More amount of pre-mixed charge is taken into the combustion chamber at rich mixture conditions and this results to higher pressure rise rate owing to higher combustion rate. The lowest RI values were obtained for E30. Ethanol has higher octane number than n-heptane resulting in more controllable auto ignition reactions. Likely, MPRR shows decreasing trend with the increase of lambda. The oxidation reactions of the fuels which have low octane number occurs more quickly. Knocking increases when the heat release seen at lower CA's. MPRR points out an important problem in internal combustion engines [22,49]. The rate of the combustion increases with the enrichment of the mixture. This situation creates an unacceptable noise problem and damage on engine parts [50]. Besides, the highest NO_x emissions are released under these conditions. Lean mixture conditions decrease the rate of combustion and MPRR. E30 fuel causes the slowest burning reactions. So, the lowest MPRR values were obtained for E30 at all lambda values. Higher reactivity of heptane increases MPRR in case of high amount in mixture fuels. The addition of ethanol to the mixture fuel reduced the MPRR by making the HCCI combustion more stable. Ethanol is an ideal fuel additive for HCCI combustion.

HCCI combustion results in high HC and CO emissions unlike compression ignition and spark ignition engines [51–53]. The main reason of HC generation is incomplete combustion. HC emissions increase due to heat losses in the regions close to the cylinder walls, fuel combining with the oil which is left in-cylinder crevices and in-cylinder

walls in the compression stroke and the re-evaporating of the fuel in the exhaust time [40–44]. The variations of the HC emissions were given at Fig. 10a. HC emissions increase due to leaner mixture conditions which result in decreasing the gas temperatures at the end of the combustion. HC decreased with the increasing of ethanol in the mixture at all lambda values. The oxygen content of the ethanol increases the combustion efficiency. BTE increases with the improvement of combustion and HC emissions decrease. CO emissions occur due to incomplete oxidation of fuel in the combustion chamber [54–56]. The main reason for this situation is low temperatures of the gasses at the end of the combustion. In the HCCI combustion takes place under the homogenous ultra lean conditions, the temperatures at the end of the combustion are low. Therefore, oxidation reactions can not be completed and CO emissions increase. The engine load increases with the enrichment of the mixture and accordingly the gas temperatures at the end of the combustion increase. So, CO emissions decrease [57,58]. The variations of CO emissions were shown at Fig. 10b. The maximum CO generation was observed for E30 for all lambda values. The higher latent heat of vaporization of ethanol causes more heat absorption from the environment. Therefore, the temperatures of the gasses at the end of the combustion decrease and CO emissions increase.

5. Conclusions

This study was carried out in a single cylinder HCCI engine with port injection system. Toluene additive was used to extend the operating range of low reactivity ethanol in HCCI engines. In this study, the operating range of all test fuels at 350 K intake air inlet temperature was determined. In addition, a detailed combustion analysis was made. The striking results of the study were as follows;

- The addition of toluene at a fixed rate (10%) to all test fuels enabled the operating range to be extended up to E20 fuel. However, the increase in the octane number of the blended fuel in the use of E30 fuel caused the majority of combustion to occur after TDC. Therefore, HCCI working range narrowed in the usage of E30 fuel. While stable HCCI burning was obtained in the range of 2.3 with E30.
- The increasing of ethanol ratio in blend fuels enabled the HCCI engine to operate at higher engine loads. HCCI combustion was obtained under extremely lean mixture conditions with the usage of high reactivity fuel (neat n-heptane, T10 and E10). The reactivity of the blending fuels has a significant effect on the operating map.
- Maximum in-cylinder pressure ($P_{\max} = 77.5$ bar) was obtained with E30 fuel which has the lowest calorific value. The high octane number of ethanol enabled HCCI combustion to be controlled. Thus, the maximum in-cylinder pressure was achieved around TDC. The

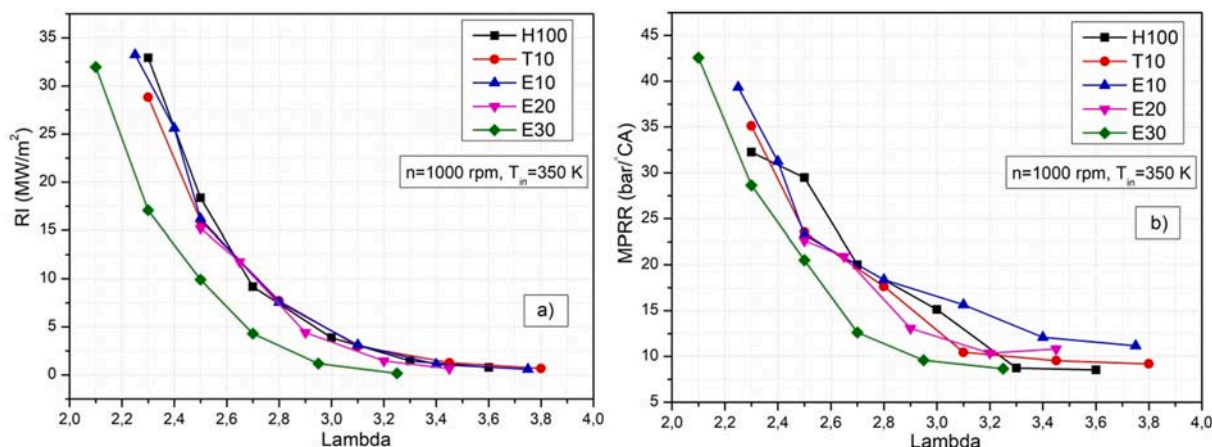


Fig. 9. The variations of a) RI and b) MPRR.

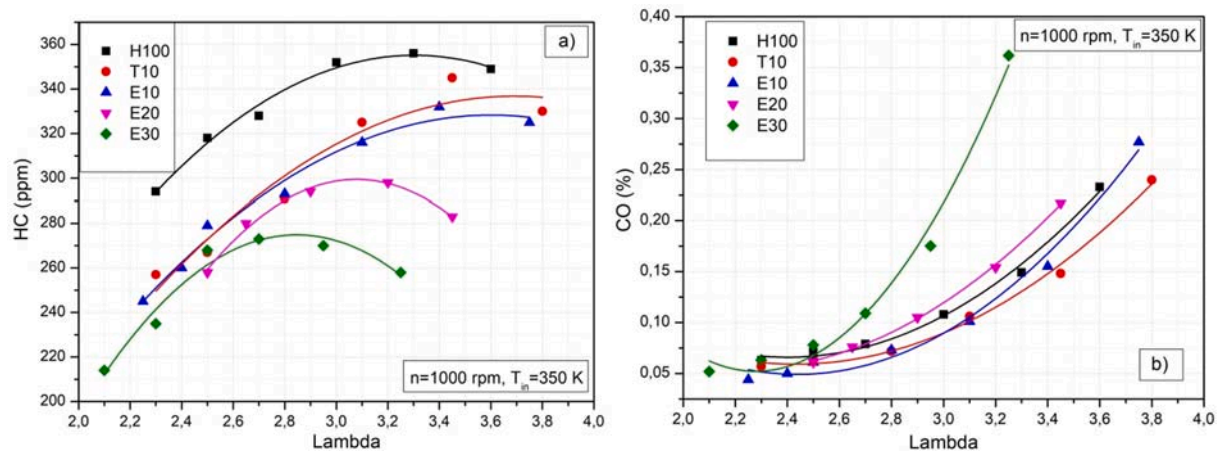


Fig. 10. The variations of a) HC and b) CO.

slower combustion reactions and the oxygen content in ethanol which improves the combustion, increased the in-cylinder pressure.

- The highest imep was obtained as 4.95 bar with the use of E30 fuel.
- Maximum brake thermal efficiency was recorded as 38.1% in the use of E30 at $\lambda = 2.95$.
- Ultra low NO_x emissions (<10 ppm) were obtained in all test fuels under stable HCCI operating conditions.
- In all test fuels, HC and CO emissions have worsened simultaneously under ultra-lean mixture conditions. Minimum HC emissions were achieved using E30 fuel, where the majority of combustion occurs around TDC.
- This work was performed on a test engine with a compression ratio of 13. The effects of toluene-ethanol blend fuels on HCCI combustion in an engine with a higher compression ratio can be studied more detailed. In addition, the effects of ethanol and toluene on HCCI combustion at higher mixing ratios at higher intake air inlet temperatures can be determined.

CRediT authorship contribution statement

Ahmet Bögrek: . : Methodology, Writing - original draft. **Can Haşimoğlu**: Supervision, Conceptualization, Methodology, Writing - original draft, Project administration. **Alper Calam**: Methodology, Software, Investigation, Writing - original draft, Writing - review & editing. **Bilal Aydoğan**: Methodology, Software, Writing - original draft, Writing - review & editing.

Declaration of Competing Interest

The authors declare that they have no known competing financial interests or personal relationships that could have appeared to influence the work reported in this paper.

References

- [1] Calam TT. Analytical application of the poly (1H-1, 2, 4-triazole-3-thiol) modified gold electrode for high-sensitive voltammetric determination of catechol in tap and lake water samples. *Int J Environ Anal Chem* 2019;99(13):1298–312. <https://doi.org/10.1080/03067319.2019.1619716>.
- [2] Calam TT. Investigation of the electrochemical behavior of phenol using 1H-1, 2, 4-triazole-3-thiol modified gold electrode and its voltammetric determination. *J Fac Eng Arch Gazi Univ* 2020;35(2):835–44. <https://doi.org/10.17341/gazimfd.543608>.
- [3] Calam TT. Electrochemical oxidative determination and electrochemical behavior of 4-nitrophenol based on an au electrode modified with electro-polymerized 3, 5-diamino-1, 2, 4-triazole film. *Electroanalysis* 2020;1(32):149–58. <https://doi.org/10.1002/elan.201900450>.
- [4] Tabanlıgil Calam T, Hasdemir E. Application of 1, 6-hexanedithiol and 1-hexane-thiol self-assembled monolayers on polycrystalline gold electrode for
- [5] Tabanlıgil Calam T, Yılmaz EB. Electrochemical determination of 8-hydroxyquinoline in a cosmetic product on a glassy carbon electrode modified with 1-amino-2-naphthol-4-sulphonic acid. *Instrument Sci Technol* 2021;49(1):1–20. <https://doi.org/10.1080/10739149.2020.1765175>.
- [6] Kocakulak T, Solmaz H. Control of pre and post transmission parallel hybrid vehicles with fuzzy logic method and comparison with other power systems. *Journal of the Faculty of Engineering and Architecture of Gazi University* 2020;35(4):2269–2286. doi:10.17341/gazimfd.709101.
- [7] Kocakulak T, Solmaz H. HCCI Menzil Arttırıcı Motor Kullanılan Seri Hibrit Bir Aracın Modellenmesi. *Gazi Üniversitesi Fen Bilimleri Dergisi Part C: Tasarım Ve Teknoloji* 2020;8(2):279–92. <https://doi.org/10.29109/gujsc.670564>.
- [8] Solmaz H, Kocakulak T. Determination of Lithium Ion Battery Characteristics for Hybrid Vehicle Models. *Int J Automot Sci Technol* 2020;4(4):264–71. <https://doi.org/10.30939/ijastech..723043>.
- [9] Okude K, Mori K, Shiino S, Moriya T. Premixed compression ignition (PCI) combustion for simultaneous reduction of NO_x and soot in diesel engine. *SAE Trans* 2004;1002–13.
- [10] Uyumaz A, Aydoğan B, Calam A, Aksoy F, Yılmaz E. The effects of diisopropyl ether on combustion, performance, emissions and operating range in a HCCI engine. *Fuel* 2020;265:116919. <https://doi.org/10.1016/j.fuel.2019.116919>.
- [11] Bahrami S, Poorghasemi K, Solmaz H, Calam A, İpci D. Effect of nitrogen and hydrogen addition on performance and emissions in reactivity controlled compression ignition. *Fuel* 2021;292:120330. <https://doi.org/10.1016/j.fuel.2021.120330>.
- [12] Ardebili SMS, Taghipoor A, Solmaz H, Mostafaei M. The effect of nano-biochar on the performance and emissions of a diesel engine fueled with fuel oil-diesel fuel. *Fuel* 2020;268:117356. <https://doi.org/10.1016/j.fuel.2020.117356>.
- [13] Ardebili SMS, Calam A, Yılmaz E, Solmaz H. A comparative analysis of the engine performance and exhaust emissions characteristics of a diesel engine fueled with Mono ethylene glycol supported emulsion. *Fuel* 2021;288:119723. <https://doi.org/10.1016/j.fuel.2020.119723>.
- [14] Sedef K, Aylanşık G, Babagıray M, Kocakulak T. Biodiesel Production from Waste Sunflower Oil and Engine Performance Tests. *Int J Automot Sci Technol* 2020;4(4): 206–12. <https://doi.org/10.30939/ijastech..770309>.
- [15] Kim DS, Lee CS. Improved emission characteristics of HCCI engine by various premixed fuels and cooled EGR. *Fuel* 2006;85(5–6):695–704. <https://doi.org/10.1016/j.fuel.2005.08.041>.
- [16] Cinar C, Uyumaz A, Solmaz H, Sahin F, Polat S, Yılmaz E. Effects of intake air temperature on combustion, performance and emission characteristics of a HCCI engine fueled with the blends of 20% n-heptane and 80% isooctane fuels. *Fuel Process Technol* 2015;130:275–81. <https://doi.org/10.1016/j.fuproc.2014.10.026>.
- [17] Yılmaz E. A Comparative Study on the Usage of RON68 and Naphtha in an HCCI Engine. *Int J Automot Sci Technol* 2020;4(2):90–7. <https://doi.org/10.30939/ijastech..721882>.
- [18] Calam A, Solmaz H, Yılmaz E, İçingür Y. Investigation of effect of compression ratio on combustion and exhaust emissions in a HCCI engine. *Energy* 2019;168: 1208–16. <https://doi.org/10.1016/j.energy.2018.12.023>.
- [19] Ardebili SMS, Solmaz H, Calam A, İpci D. Modelling of performance, emission, and combustion of an HCCI engine fueled with fuel oil-diethylether fuel blends as a renewable fuel. *Fuel* 2021;290:120017. <https://doi.org/10.1016/j.fuel.2020.120017>.
- [20] Dec JE, Yang Y. Boosted HCCI for high power without engine knock and with ultra-low NO_x emissions-using conventional gasoline. *SAE Int J Engines* 2010;3(1): 750–67.
- [21] Andreea MM, Cheng WK, Kenney T, Yang J. On HCCI engine knock. *SAE Trans* 2007:355–63.

- [22] Hou J, Qiao X, Wang Z, Liu W, Huang Z. Characterization of knocking combustion in HCCI DME engine using wavelet packet transform. *Appl Energy* 2010;87(4):1239–46. <https://doi.org/10.1016/j.apenergy.2009.06.014>.
- [23] Calam A. Study on the combustion characteristics of acetone/n-heptane blend and RON50 reference fuels in an HCCI engine at different compression ratios. *Fuel* 2020;271:117646. <https://doi.org/10.1016/j.fuel.2020.117646>.
- [24] Sjöberg M, Dec JE, Cernansky NP. Potential of thermal stratification and combustion retard for reducing pressure-rise rates in HCCI engines, based on multi-zone modeling and experiments. *SAE Trans* 2005:236–51.
- [25] Polat S, Uyumaz A, Solmaz H, Yilmaz E, Topgül T, Yücesu HS. A numerical study on the effects of EGR and spark timing to combustion characteristics and NO_x emission of a GDI engine. *Int J Green Energy* 2016;13(1):63–70. <https://doi.org/10.1080/15435075.2014.909361>.
- [26] Polat S, Solmaz H, Uyumaz A, Calam A, Yilmaz E, Serdar YH. An experimental research on the effects of negative valve overlap on performance and operating range in a homogeneous charge compression ignition engine with RON40 and RON60 fuels. *J Eng Gas Turbines Power* 2020;142(5). <https://doi.org/10.1115/1.4046695>.
- [27] Fathi M, Saray RK, Checkel MD. The influence of Exhaust Gas Recirculation (EGR) on combustion and emissions of n-heptane/natural gas fueled Homogeneous Charge Compression Ignition (HCCI) engines. *Appl Energy* 2011;88(12):4719–24. <https://doi.org/10.1016/j.apenergy.2011.06.017>.
- [28] Calam A, Aydoğan B, Halis S. The comparison of combustion, engine performance and emission characteristics of ethanol, methanol, fusel oil, butanol, isopropanol and naphtha with n-heptane blends on HCCI engine. *Fuel* 2020;266:117071. <https://doi.org/10.1016/j.fuel.2020.117071>.
- [29] Li G, Zhang C, Zhou J. Study on the knock tendency and cyclical variations of a HCCI engine fueled with n-butanol/n-heptane blends. *Energy Convers Manage* 2017;133:548–57. <https://doi.org/10.1016/j.enconman.2016.10.074>.
- [30] Bahri B, Shahbakhti M, Aziz AA. Real-time modeling of ringing in HCCI engines using artificial neural networks. *Energy* 2017;125:509–18. <https://doi.org/10.1016/j.energy.2017.02.137>.
- [31] Wang Z, Liu H, Ma X, Wang J, Shuai S, Reitz RD. Homogeneous charge compression ignition (HCCI) combustion of polyoxymethylene dimethyl ethers (PODE). *Fuel* 2016;183:206–13. <https://doi.org/10.1016/j.fuel.2016.06.033>.
- [32] Bahri B, Aziz AA, Shahbakhti M, Said MF. Understanding and detecting misfire in an HCCI engine fuelled with ethanol. *Appl Energy* 2013;108:24–33. <https://doi.org/10.1016/j.apenergy.2013.03.004>.
- [33] Cinar C, Uyumaz A, Solmaz H, Topgul T. Effects of valve lift on the combustion and emissions of a HCCI gasoline engine. *Energy Convers Manage* 2015;94:159–68. <https://doi.org/10.1016/j.enconman.2015.01.072>.
- [34] Starck L, Lecoite B, Forti L, Jeuland N. Impact of fuel characteristics on HCCI combustion: Performances and emissions. *Fuel* 2010;89(10):3069–77. <https://doi.org/10.1016/j.fuel.2010.05.028>.
- [35] Machrafi H, Cavadias S, Gilbert P. An experimental and numerical analysis of the HCCI auto-ignition process of primary reference fuels, toluene reference fuels and diesel fuel in an engine, varying the engine parameters. *Fuel Process Technol* 2008;89(11):1007–16. <https://doi.org/10.1016/j.fuproc.2008.03.007>.
- [36] Lee CF, Wu Y, Wu H, Shi Z, Zhang L, Liu F. The experimental investigation on the impact of toluene addition on low-temperature ignition characteristics of diesel spray. *Fuel* 2019;254:115580. <https://doi.org/10.1016/j.fuel.2019.05.163>.
- [37] Maurya RK, Agarwal AK. Experimental study of combustion and emission characteristics of ethanol fuelled port injected homogeneous charge compression ignition (HCCI) combustion engine. *Appl Energy* 2011;88(4):1169–80. <https://doi.org/10.1016/j.apenergy.2010.09.015>.
- [38] Zhang S, Lee TH, Wu H, Pei J, Wu W, Liu F, et al. Experimental and kinetic studies on laminar flame characteristics of acetone-butanol-ethanol (ABE) and toluene reference fuel (TRF) blends at atmospheric pressure. *Fuel* 2018;232:755–68. <https://doi.org/10.1016/j.fuel.2018.05.150>.
- [39] Gawale GR, Srinivasulu GN. Experimental investigation of ethanol/diesel and ethanol/biodiesel on dual fuel mode HCCI engine for different engine load conditions. *Fuel* 2020;263:116725. <https://doi.org/10.1016/j.fuel.2019.116725>.
- [40] Polat S. An experimental study on combustion, engine performance and exhaust emissions in a HCCI engine fuelled with diethyl ether–ethanol fuel blends. *Fuel Process Technol* 2016;143:140–50. <https://doi.org/10.1016/j.fuproc.2015.11.021>.
- [41] Swan K, Shahbakhti M, Koch CR. Predicting start of combustion using a modified knock integral method for an HCCI engine. *SAE Trans* 2006:611–20.
- [42] Heywood JB. *Combustion engine fundamentals*. 1^a Edição. Estados Unidos. 1988.
- [43] Zhao F, Asmus T. N., Assanis D. N., Dec J. E., Eng J. A., & Najt P. M. Homogeneous charge compression ignition (HCCI) engines (No. PT-94). SAE Technical Paper, 2003.
- [44] Solmaz H. A comparative study on the usage of fusel oil and reference fuels in an HCCI engine at different compression ratios. *Fuel* 2020;273:117775. <https://doi.org/10.1016/j.fuel.2020.117775>.
- [45] Polat S, Solmaz H, Yilmaz E, Calam A, Uyumaz A, Yücesu HS. Mapping of an HCCI engine using negative valve overlap strategy. *Energy Sources Part A* 2020;42(9):1140–54. <https://doi.org/10.1080/15567036.2019.1602224>.
- [46] Lü X, Hou Y, Zu L, Huang Z. Experimental study on the auto-ignition and combustion characteristics in the homogeneous charge compression ignition (HCCI) combustion operation with ethanol/n-heptane blend fuels by port injection. *Fuel* 2006;85(17–18):2622–31. <https://doi.org/10.1016/j.fuel.2006.05.003>.
- [47] Saxena S, Schneider S, Aceves S, Dibble R. Wet ethanol in HCCI engines with exhaust heat recovery to improve the energy balance of ethanol fuels. *Appl Energy* 2012;98:448–57. <https://doi.org/10.1016/j.apenergy.2012.04.007>.
- [48] da Costa RBR, Valle RM, Hernández JJ, Malaquias ACT, Coronado CJ, Pujatti FJP. Experimental investigation on the potential of biogas/ethanol dual-fuel spark-ignition engine for power generation: Combustion, performance and pollutant emission analysis. *Appl Energy* 2020;261:114438. <https://doi.org/10.1016/j.apenergy.2019.114438>.
- [49] Wildman C, Scaringe RJ, & Cheng W. On the maximum pressure rise rate in boosted HCCI operation (No. 2009-01-2727). SAE Technical Paper, 2009.
- [50] Aydoğan B. Combustion characteristics, performance and emissions of an acetone/n-heptane fuelled homogenous charge compression ignition (HCCI) engine. *Fuel* 2020;275:117840. <https://doi.org/10.1016/j.fuel.2020.117840>.
- [51] Easley WL, Agarwal A, Lavoie GA. Modeling of HCCI combustion and emissions using detailed chemistry. *SAE Trans* 2001:1045–61.
- [52] Dec JE, Sjöberg M. A parametric study of HCCI combustion—the sources of emissions at low loads and the effects of GDI fuel injection. *SAE Trans* 2003:1119–41.
- [53] Aydoğan B. An experimental examination of the effects of n-hexane and n-heptane fuel blends on combustion, performance and emissions characteristics in a HCCI engine. *Energy* 2020;192:116600. <https://doi.org/10.1016/j.energy.2019.116600>.
- [54] Aydoğan B. Experimental investigation of tetrahydrofuran combustion in homogenous charge compression ignition (HCCI) engine: Effects of excess air coefficient, engine speed and inlet air temperature. *J Energy Inst* 2020;93:1163–76. <https://doi.org/10.1016/j.joei.2019.10.009>.
- [55] Ardebili SMS, Solmaz H, Mostafaei M. Optimization of fusel oil–Gasoline blend ratio to enhance the performance and reduce emissions. *Appl Therm Eng* 2019;148:1334–45. <https://doi.org/10.1016/j.applthermaleng.2018.12.005>.
- [56] Yilmaz E, Solmaz H, Polat S, Uyumaz A, Şahin F, Salman MS. Preparation of diesel emulsion using auxiliary emulsifier mono ethylene glycol and utilization in a turbocharged diesel engine. *Energy Convers Manage* 2014;86:973–80. <https://doi.org/10.1016/j.enconman.2014.06.033>.
- [57] Aceves SM, Flowers DL, Westbrook CK, Smith JR, Pitz W, Dibble R, et al. A multi-zone model for prediction of HCCI combustion and emissions. *SAE Trans* 2000:431–41.
- [58] Solmaz H, Yamık H, İcिंगür Y, Calam A. Investigation of the effects of civil aviation fuel Jet al blends on diesel engine performance and emission characteristics. *Indian J Eng Mater Sci* 2014;21(2):200–6.